NASA TND-1064

TECHNICAL NOTE

D-1064

MEASUREMENTS OF SHEATH CURRENTS AND EQUILIBRIUM POTENTIAL ON THE EXPLORER VIII SATELLITE (1960ξ)

R. E. Bourdeau, J. L. Donley,
G. P. Serbu and E. C. Whipple, Jr.

Goddard Space Flight Center
Greenbelt, Maryland

NATIONAL AERONAUTICS AND SPACE ADMINISTRATION
WASHINGTON July 1961

MEASUREMENTS OF SHEATH CURRENTS AND EQUILIBRIUM POTENTIAL ON THE EXPLORER VIII SATELLITE (1960 ξ)

by
R. E. Bourdeau, J. L. Donley,
G. P. Serbu and E. C. Whipple, Jr.
Goddard Space Flight Center

D-1064

SUMMARY

Experimental data were obtained from the Explorer VIII satellite on five parameters pertinent to the problem of the interaction of space vehicles with an ionized atmosphere. The five parameters are: photoemission current due to electrons emitted from the satellite surfaces as a result of solar radiation; electron and positive ion currents due to the diffusion of charged particles from the medium to the spacecraft; the vehicle potential relative to the medium, and the ambient electron temperature. Included in the experimental data is the aspect dependence of the photoemission and diffusion currents. On the basis of the observations, certain characteristics of the satellite's plasma sheath are postulated.

CONTENTS

MEASUREMENTS OF SHEATH CURRENTS AND EQUILIBRIUM POTENTIAL ON THE EXPLORER VIII SATELLITE (1960 ξ)

by
R. E. Bourdeau, J. L. Donley,
G. P. Serbu and E. C. Whipple, Jr.
Goddard Space Flight Center

INTRODUCTION

This discussion is concerned with one type of interaction between a space vehicle and an ionized atmosphere. Specifically, it deals with the equilibrium potential of the Explorer VIII satellite, and the current exchange between this spacecraft and the ionosphere. The experimental data presented herein are fundamental to the characteristics of the plasma sheath surrounding a space vehicle. We are dealing, then, with an interaction confined to the proximity of the body. Since all disturbances must begin right at the body itself, these data may be found useful in evaluating other types of interactions that have been postulated.

Both the characteristics of the ionosphere and those of the space vehicle contribute to their mutual interaction. For an orbiting satellite, the sheath properties are determined by the following factors:

Parameters of the Undisturbed Ionosphere:

1. the ambient electron temperature, T_e;
2. the random electron current density, J_e;
3. the random ion current density, J_+;
4. the magnetic field, B.

Factors Due to the Presence of the Satellite:

1. radio-frequency fields used for telemetry transmissions;
2. the conductivity of the surface;
3. the photoemission current density (J_p) due to solar radiation;
4. the satellite motion.

For a conducting body at rest where RF and magnetic fields and solar radiation may be neglected, the equilibrium potential is given by:

$$\phi_0 = \frac{-kT_e}{e} \ln \frac{J_e}{J_+} , \tag{1}$$

where k is Boltzmann's constant and e the electronic charge. Since $J_e >> J_+$, ϕ will be negative; this will result in a positive ion sheath with a thickness related to T_e and to the electron concentration N_e.

Consider now the factors introduced by the presence of the satellite. It is known that antennas radiating RF fields can, by a rectifying process, cause a larger negative potential than would be expected from Equation 1. However, experimental observations made from rockets (Reference 1) during RF silence have been compared with data taken in the same flight during RF transmissions. These data show that for the amount of power (100 mw) and the frequency (108 Mc) used by the Explorer VIII telemetry system, the RF field effect due to telemetry transmissions can be neglected.

The satellite motion affects the sheath in the following manner. Since the satellite velocity greatly exceeds that of the positive ions, the random ion current is essentially incident over that portion of the satellite surface projected in the direction of motion. The electron current also should be greatest at the forward surface, although the effect will be smaller because of the higher thermal velocities of the electrons.

The electron current is also affected by the magnetic field, as Beard and Johnson (Reference 2) have described. The motion of the satellite with velocity v through the magnetic field produces an induced potential that is a function of position on the satellite surface,

$$\phi = \phi_0 + (\vec{V} \times \vec{B}) \cdot \vec{d} \tag{2}$$

where ϕ_0 would be the satellite potential with no magnetic field, and $\vec{d}$ is the vector distance of any point on the surface from the satellite center. A satellite potential of ϕ_0 will be measured at all points that lie on a plane through the satellite center perpendicular to $\vec{V} \times \vec{B}$. All other points will be more positive or negative than ϕ_0 as they are situated on one side of this plane or the other. The maximum electron current would be expected where ϕ is most positive, i.e., near the point corresponding to the direction $\vec{V} \times \vec{B}$.

The photoemission current density J_p tends to make ϕ_0 more positive. At low electron concentrations photoemission can predominate, resulting in a positive ϕ_0 and a sheath containing electrons.

If the effects of the magnetic field and satellite velocity on the electron current can be neglected, the following expression for the satellite potential is valid:

$$\phi_0 = -\frac{kT_e}{e} \ln \frac{J_e S}{\int J_+ dS + \int J_p dS} \tag{3}$$

where the integration is over the satellite surface S. To take the electron current variations into account, it is necessary to return to the fundamental equation for current balance:

$$\int J_e \, dS = \int J_+ dS + \int J_p dS \, . \tag{4}$$

This report will present experimental values — obtained from the Explorer VIII satellite — of the electron diffusion current i_e, the ion diffusion current i_+, and the photoemission current i_p, as functions of the orientation of those points relative to the velocity, solar, and magnetic field vectors. Also presented will be measured values of ϕ and T_e. These experimental observations will then be used to postulate a qualitative model of the plasma sheath and a quantitative model of the current exchange between satellite and medium.

D-1004

THE EXPLORER VIII SATELLITE

Explorer VIII was launched on November 3, 1960, from Cape Canaveral, Florida, into an orbit with an inclination of 50 degrees to the equator, a perigee of 425 kilometers, and an apogee of 2300 kilometers. Its planned active life was two months. The primary mission of this Ionosphere Direct Measurements Satellite, which is only incidental to this report, was the in-situ measurement of electron density and temperature and of positive ion concentration and mass.

A photograph of the satellite, highlighting the characteristics pertinent to this discussion, is presented in Figure 1. The aluminum shell, consisting of two truncated cones joined at the equator by a short cylinder, is 30 inches in diameter at the equator and 30 inches high. Non-conductive thermal coatings are located on both cones in a pattern conducive to the maintenance of an equipotential surface. Two ten-foot wires, shown retracted in the photograph served as a shortened dipole for an RF impedance experiment designed to measure N_e. A combined solar-horizon seeker provided supporting information on the satellite orientation.

Data from only four of the satellite's many sensors are considered in this presentation. They are:

1. an ion current monitor, responsive only to the incoming positive ions;
2. an electron current monitor, responsive to the sum of the incoming electron current and outgoing photoemission current;
3. a total current monitor, responsive to all three types of current;
4. an electron temperature probe, responsive only to electron current and which measures φ and T_e.

The locations of these four sensors relative to the aspect sensor are shown in Figure 2. All but the electron temperature probe are centered on the equator. The latter sensor is positioned near the forward end of the spin axis as shown in Figure 1.

In order to evaluate in detail the simultaneous effect of all the sheath-influencing factors cited in the introduction, a single set of conditions was chosen wherein favorable satellite orientation permits clear delineation of the dependency of the ion, electron, and photoemission currents on the location of the velocity, solar, and magnetic field vectors. Consequently, all of the reported data will be for the orientation described by Figure 3. Of major importance is the fact that the velocity and solar vectors are separated by 159 degrees. This permits separate scanning of the solar and velocity dependent quantities as the satellite spins. The solar elevation angle was 33 degrees on the upper cone and the velocity vector depression angle was 15 degrees on the lower cone. All the data were acquired within two minutes of 22:57 UT on 27 November 1960, at which time the satellite's altitude was 1000 kilometers and its geographic coordinates were 33°N and 84°E. The spin rate was 21.4 rpm at this time.

MEASURED VALUES OF POSITIVE ION CURRENT

The positive ion current flowing from the ionosphere to the satellite was monitored by a sensor shown schematically in Figure 4. The sensor is constructed in planar geometry and contains three parallel electrodes. The outermost grid is flush with and electrically connected to the satellite skin. The inner grid is biased negatively to suppress photoemission from the collector and to remove incoming electron current from the measured collector current. This collector current i_+ is related to $(i_+)_s$, the current incident at the skin, by

$$i_+ = \alpha_+(i_+)_s \tag{5}$$

where α_+ is the combined electrical transparency of the two grids for positive ions.

The experimental collector current is plotted in Figure 5 as a function of the azimuth angle of the sensor relative to the velocity and solar vectors. The absence of a current

when the sensor is pointed at the sun is proof that photoemission from the collector has been successfully suppressed. The behavior of i_+ relative to the velocity vector is in good agreement with that predicted by Whipple (Reference 3) in the following general equation which takes into account all values of the satellite-to-ion velocity ratio:

$$i = \alpha NeA \left[V \cos\theta \left(\frac{1}{2} + \frac{1}{2} \operatorname{erf} x \right) + \frac{a \exp(-x^2)}{2\sqrt{\pi}} \right], \quad . \tag{6}$$

where $x = (V \cos\theta/a) - \sqrt{|\phi|e/kT}$, and where A is the area of the collector, N the particle concentration, a the most probable thermal velocity of the particle, and θ the angle between the sensor and the velocity vector. This expression has been derived for plane geometry and is valid for either ions or electrons if the appropriate values and signs for the symbols are observed. For angles less than 45 degrees in Figure 5, the observed currents are fitted by the reduced equation:

$$i_+ = \alpha_+ AN_+ eV \cos\theta . \tag{7}$$

With an in-flight calibration of the combined electrical transparency of the two grids (92 percent), a value for N_+ of $1.3 \times 10^4/cm^3$ is computed. This is consistent with electron concentrations obtained from the RF impedance probe experiment also carried on Explorer VIII. Ionosonde data taken at this geographical position and at this time yield an electron density of 7×10^5 electrons/cm^3 at an altitude of about 300 kilometers. The positive ion concentration measured from the satellite agrees with this value, assuming an ionospheric model with a neutral gas scale height of 60 kilometers, diffusive equilibrium, and a predominant O^+ constituent.

One important qualitative conclusion related to sheath characteristics can be drawn from Figure 5: The absence of a positive ion current on the side away from the velocity vector is definite experimental evidence for an electron sheath immediately adjoining the vehicle at this location.

In Figure 6 are plotted values of ion current density computed from i_+/A as a function of the total angle relative to the velocity vector. The solid line is a theoretical curve based on Equation 6. The agreement between the observed currents and the equation is evident. However, to get agreement for angles greater than 45 degrees, a value of 3.6×10^5 cm/sec had to be used in the equation for the most probable ion thermal velocity. This value corresponds to an anomalously high ion temperature if only O^+ is assumed, but is reasonable if there is a significant amount of H^+; the implication is that at 1000 kilometers the satellite is near the transition region between the upper ionosphere and the protonosphere. Another possible explanation is that Equation 6 should be modified to account for the effect on the positive ion collection of electric fields penetrating the sheath at the sides of the satellite (Reference 4).

MEASURED VALUES OF ELECTRON CURRENT

A sensor responsive to the sum of the incoming electron current and the outgoing photoemission current is illustrated schematically in Figure 7. It is mechanically identical to the ion current monitor but differs electrically in that the inner grid is biased positively rather than negatively. The positive bias serves to remove the incoming ion current from the measured collector current. The collector current is given by

$$i = i_e + i_p = \alpha_e (i_e)_s + \alpha_p (i_p)_s , \tag{8}$$

where α_e and α_p are the respective grid transparencies.

The experimental collector current is plotted in Figure 8 as a function of aspect. The current has its maximum positive value (photoemission) when the azimuth angle of the sensor relative to the sun is zero. As was postulated in the introduction, the incoming electron current should be a function of the sensor orientation relative to both the velocity and the magnetic field vectors. In this case, the maximum electron current on the shaded side is observed when the angle between the sensor and the cross-product of the velocity and magnetic fields vectors ($\vec{V} \times \vec{B}$) approaches a minimum. This is as expected because at this time during a spin period the surface near this sensor location would be at its most positive point.

MEASURED VALUES OF TOTAL CURRENT

The total current to the satellite was measured at its equator by the sensor illustrated in Figure 9. It consists simply of a collector flush with and insulated from the satellite skin. This collector current is given by

$$i = i_t = (i_e)_s + (i_+)_s + (i_p)_s . \tag{9}$$

It represents then, the sum of the effects of Figures 5 and 8, except that the overall amplitude of each component is larger since no grid transparencies are involved.

The total current at the point of measurement is plotted as a function of aspect in Figure 10. It is in definite agreement with the predominant features of the graphs in Figures 5 and 8. Specifically, the current peaks in the positive direction when the solar angle is zero because of photoemission. The current peaks again in the positive direction for a velocity azimuth angle near zero. The peak here is due to the "ram effect" upon which the positive ion current is largely dependent. The displacement from the zero angle point is due to the influence of the electron current in this region. Finally, a peak current in the direction of an incoming electron current occurs when the angle between

the sensor and the cross-product of the velocity and magnetic field vectors ($\vec{V} \times \vec{B}$) approaches a minimum.

The satellite spin permits examination of the separate behavior of each of the three currents comprising the total current curve. This in turn makes it possible, by comparison of Figure 10 with Figures 5 and 8, to assign an electrical transparency to the grids used in the ion and electron current monitors. This in-flight calibration shows that the combined electrical transparency of two parallel grids for positive ions is approximately the optical transparency. On the other hand, the electrical transparency for electrons is only about 30 percent of the optical transparency — an important observation in evaluating electron temperature data, which are discussed in a later section.

A significant quantitative value derived from Figure 10 is the measured value of the photoemission current density (5×10^{-9} ampere/cm^2) taken right at the vehicle surface for a minimum solar angle. This value can be compared with the random electron current density computed from ionospheric models to predict an approximate altitude at which the spacecraft potential can become positive. For most ionospheric models, this should occur at about 4000 kilometers, not too far above the apogee altitude of Explorer VIII.

MEASURED VALUES OF ELECTRON TEMPERATURES AND EQUILIBRIUM POTENTIAL

The sensor illustrated schematically in Figure 11 was used on a time-sharing basis to monitor alternately the incoming electron current at the sensor location and, in the other half of its duty cycle, electron temperature and equilibrium potential. The sensor consists of two electrodes, a grid, and a collector. The collector is biased positively to remove photoemission and incoming ion current from the measured collector current. During one time phase the grid is kept at the skin potential, thus permitting a measurement of the incoming electron current as a function of aspect. During the other time phase the grid potential relative to the satellite skin is varied from -1.2 to +8 volts to obtain ϕ and T_e. The period of the grid voltage sweep is kept small (0.2 seconds) so that the collector current can be studied as a function of the grid voltage for small changes in orientation. At the satellite spin rate, it was possible to obtain a volt-ampere curve for a change in orientation of about 25 degrees.

Figure 12 is a typical volt-ampere curve taken during the phase when the potential of the grid relative to the satellite skin was varied in accordance with the waveform illustrated in Figure 11. The shape of the electron current curve, plotted on a logarithmic scale, is in good agreement with Langmuir probe theory. Two distinct slopes are apparent in the regions where the grid is below and above the plasma potential. The slope of the

curve when the grid potential is negative is a measure of the electron temperature. The satellite potential is generally taken as the negative value of either the point where the curve departs from this slope, or the intersection point of the two slopes. For the illustrated curve, an electron temperature of 1800° ± 300°K and a satellite potential between 0 and -0.15 volt is obtained. The error quoted in the temperature is due to the limited resolution.

Additional volt-ampere curves taken at this time for different sensor orientations are not presented here. These other curves show that as the satellite spins, the same values of electron temperature are obtained. The major difference is the current read at the plasma potential. These values are consistent with the electron current behavior when the grid is maintained at zero volts as shown in Figure 13.

The large scatter of points in Figure 13 as compared to all the previous graphs occurs because the electrometer sensitivity range is such that the input voltage to the telemetry system is small. The scatter is due, therefore, to random fluctuations of the telemetry subcarrier at low signal levels. Despite this difficulty, it is apparent that the electron current peaks when the velocity vector azimuth angle is zero. From this observation, together with an examination of the relative values of V and ϕ in Equation 6, it can be concluded that the potential of the upper cone relative to the medium must be close to zero as indicated above or can even become positive as the satellite spins.

Figure 14, which depicts the orientation of the satellite with respect to the magnetic and velocity vectors, verifies this implication. The sensor on the upper cone always remains on the "positive" half of the satellite, i.e., the side that is positive with respect to ϕ_0. Moreover, the change in the distance from the ϕ_0 plane is only 24 centimeters, corresponding to a change in potential of about 0.04 volt. In contrast, the potential on the equator changes by at least 0.14 volt and becomes more negative than ϕ_0. (Values of 7.4×10^5 cm/sec for V and 0.30 gauss for B were used in the above computation). Note also that the electron current in Figure 13 is consistently larger than that to the sensor on the equator, as would be expected.

It remains to point out that these conclusions regarding the potential are necessary but not sufficient to explain Figure 13. The observed current modulation requires a lower electron temperature than the 1800°K discussed in the preceding paragraphs. As was suggested previously, there is evidence that the electrical transparency of the grids to electrons is a function of the electron energy, the fast electrons getting through more readily. This situation would tend to enhance any current modulation present, and it is suggested that this is in fact occurring here. A changing grid transparency may also affect the determination of temperature. A thorough evaluation of the grid transparency effect on the electron temperature measurement has not yet been completed.

SHEATH CHARACTERISTICS POSTULATED FROM EXPERIMENTAL OBSERVATIONS

It is concluded that the experimental data from the various sensors are mutually consistent. These data can be used to postulate a qualitative model of the sheath characteristics and a quantitative model of the current exchange between the satellite and the medium.

First, the value of the satellite potential on the upper cone is between 0 and -0.15 volt. The satellite surface is not equipotential. The motion of the satellite through the magnetic field causes an induced potential, so that the potential is very close to zero or positive in the $\vec{V} \times \vec{B}$ direction and correspondingly more negative at the other end.

The potential distribution on the surface has a marked effect on the observed electron current, with most electrons incident at the more positive end. It should be noted that there was a net electron current to the skin even when the current flow was perpendicular to the magnetic field. A qualitative model of the sheath surrounding the satellite is illustrated in Figure 15, showing also the effects of solar and velocity vector orientations on the various current exchanges. The electron current shows a ram effect due to the satellite motion if the frontal surface is favorably situated with respect to the more positive end of the satellite.

The positive ion current density is a function only of the angle between the surface normal and the satellite velocity vector. The absence of this current behind the satellite indicates that there is an electron sheath or wake adjoining the rear surface. If it is assumed that the wake is in the form of a cone, its size may be estimated from the ratio of satellite to ion velocities and the satellite diameter. In this case the cone has a half-angle of about 25 degrees and extends back a distance of about one satellite radius. A positive ion sheath surrounds the front of the satellite and should envelope both the satellite and the electron wake. The thickness of the ion sheath would be comparable to one Debye length, which is computed to be 2.5 centimeters.

Finally, there is a photoemission current on the satellite surfaces facing the sun. This current is important in considering the current balance to the satellite and thus the equilibrium potential. However, photoemission does not appear to disturb the sheath adjacent to the emitting surface.

The sheath model illustrated in Figure 15 is for an altitude of 1000 kilometers. The measured positive ion density is $1.3 \times 10^4/cm^3$. A neutral gas scale height of 60 kilometers, corresponding to a temperature of about 1100°K, is indicated by comparison of this N^+ with ionosonde data. An electron temperature of $1800° \pm 300°K$ was measured by the electron temperature probe. However, this value could be influenced by the effect on the probe's grid transparency of a changing electron retarding potential; the percentage

modulation of the electron current by the satellite velocity indicates a somewhat lower value for T_e. The behavior of the positive ion current at the satellite sides suggest the possibility that the transition region between the ionosphere and the protonosphere is near 1000 kilometers.

ACKNOWLEDGMENTS

Dr. R. C. Waddell and Mr. W. J. Archer of the Goddard Space Flight Center were responsible for the instrumentation associated with the experiments. Mr. C. R. Hamilton of GSFC acted as project coordinator. Also acknowledged are the helpful discussions with Dr. S. J. Bauer of GSFC and Dr. C. A. Pearse of the Naval Research Laboratory.

REFERENCES

1. Smith, L. G., Private Communication
2. Beard, B. D., and Johnson, F. S., "Charge and Magnetic Field Interaction with Satellites," J. Geophys. Res. 65(1):1-7, January 1960
3. Whipple, E. C., "The Ion-Trap Results in 'Exploration of the Upper Atmosphere with the Help of the Third Soviet Sputnik'," Proc. I.R.E. 47(11):2023-2024, November 1959
4. Schulz, G. J., and Brown, S. C., "Microwave Study of Positive Ion Collection by Probes," Phys. Rev. 98(6):1642-1649, June 1955

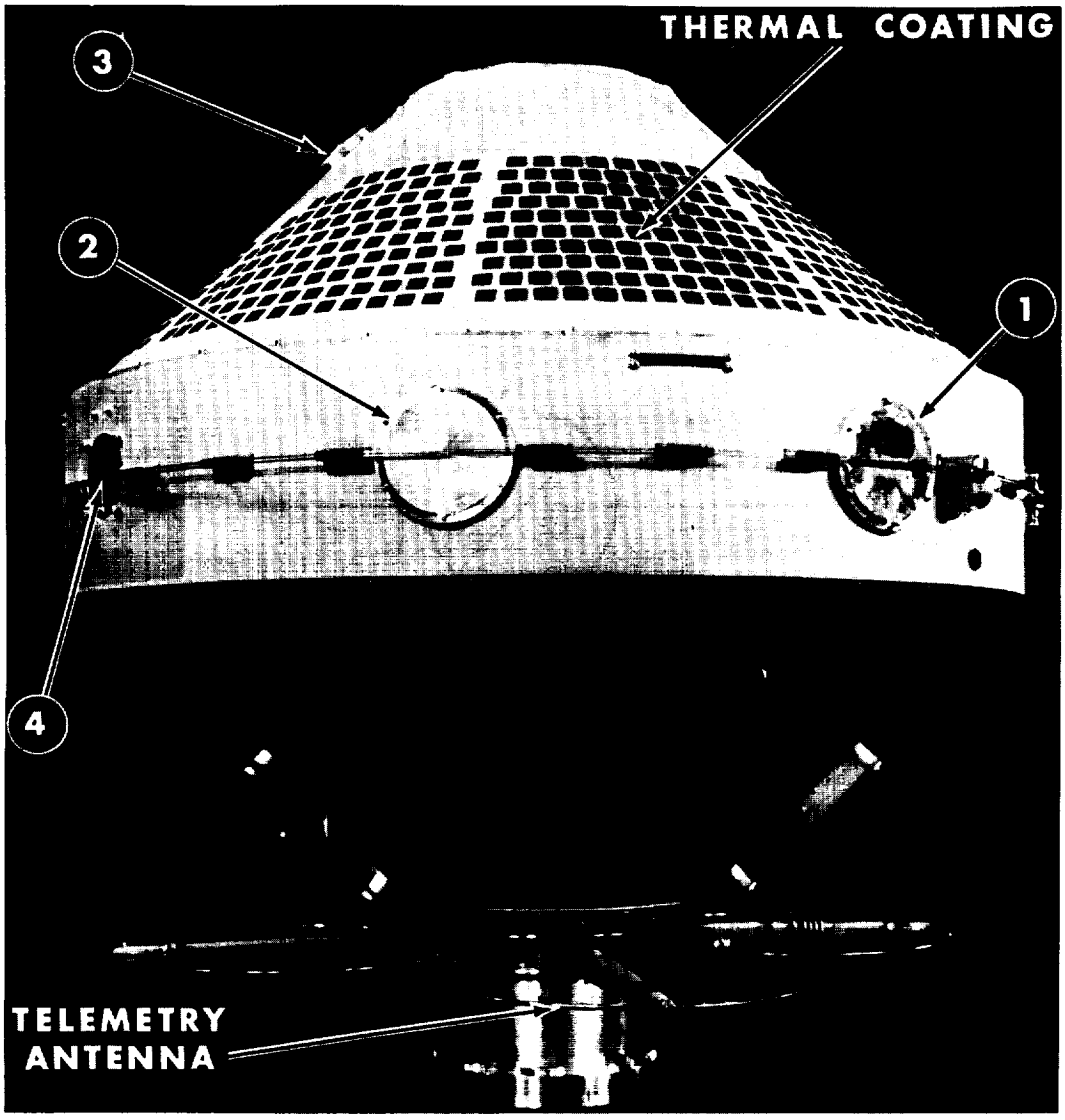

(1) ELECTRON CURRENT MONITOR
(2) TOTAL CURRENT MONITOR
(3) ELECTRON TEMPERATURE PROBE
(4) ASPECT SENSOR

Figure 1 - Ionosphere Direct Measurements Satellite (Explorer VIII)

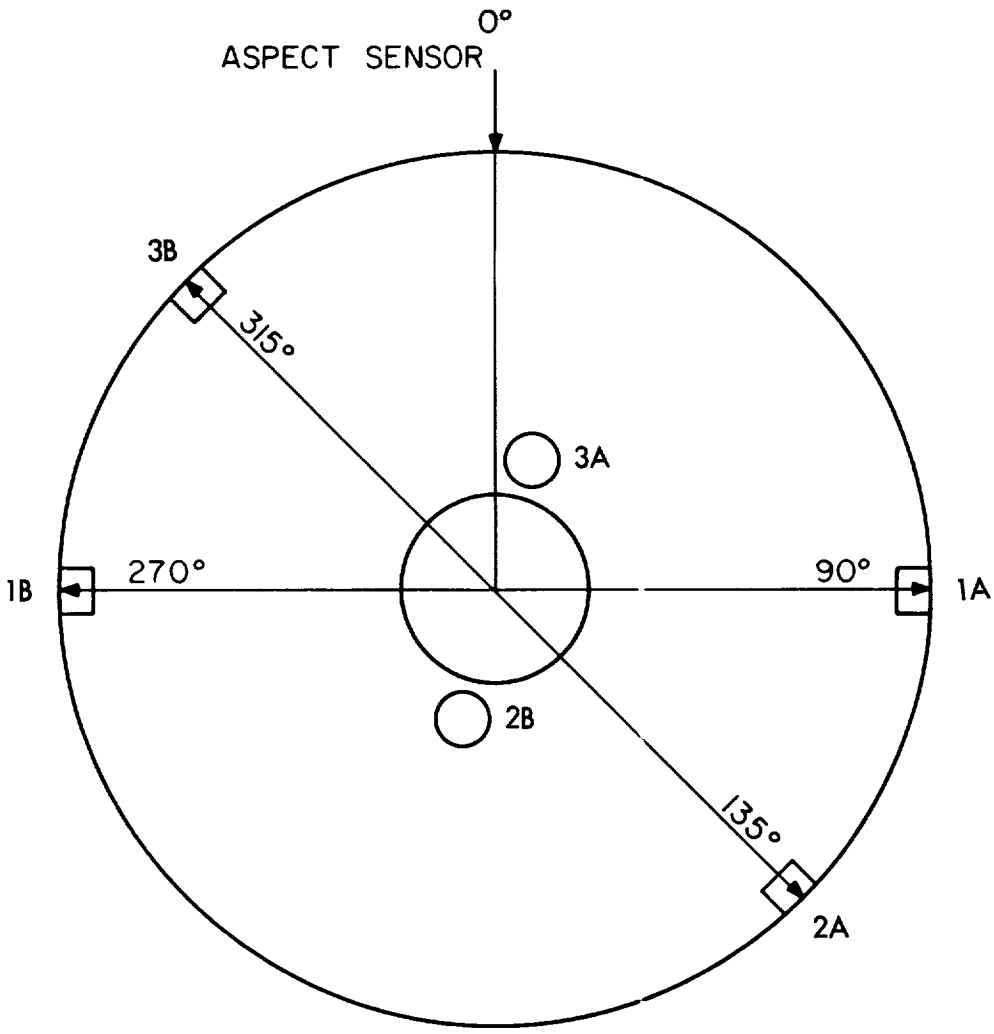

1A ION CURRENT MONITOR
1B ELECTRON CURRENT MONITOR
2A RETARDING POTENTIAL PROBE
2B ELECTRON TEMPERATURE PROBE
3A ELECTRON TEMPERATURE PROBE
3B TOTAL CURRENT MONITOR

Figure 2 - Sensor locations

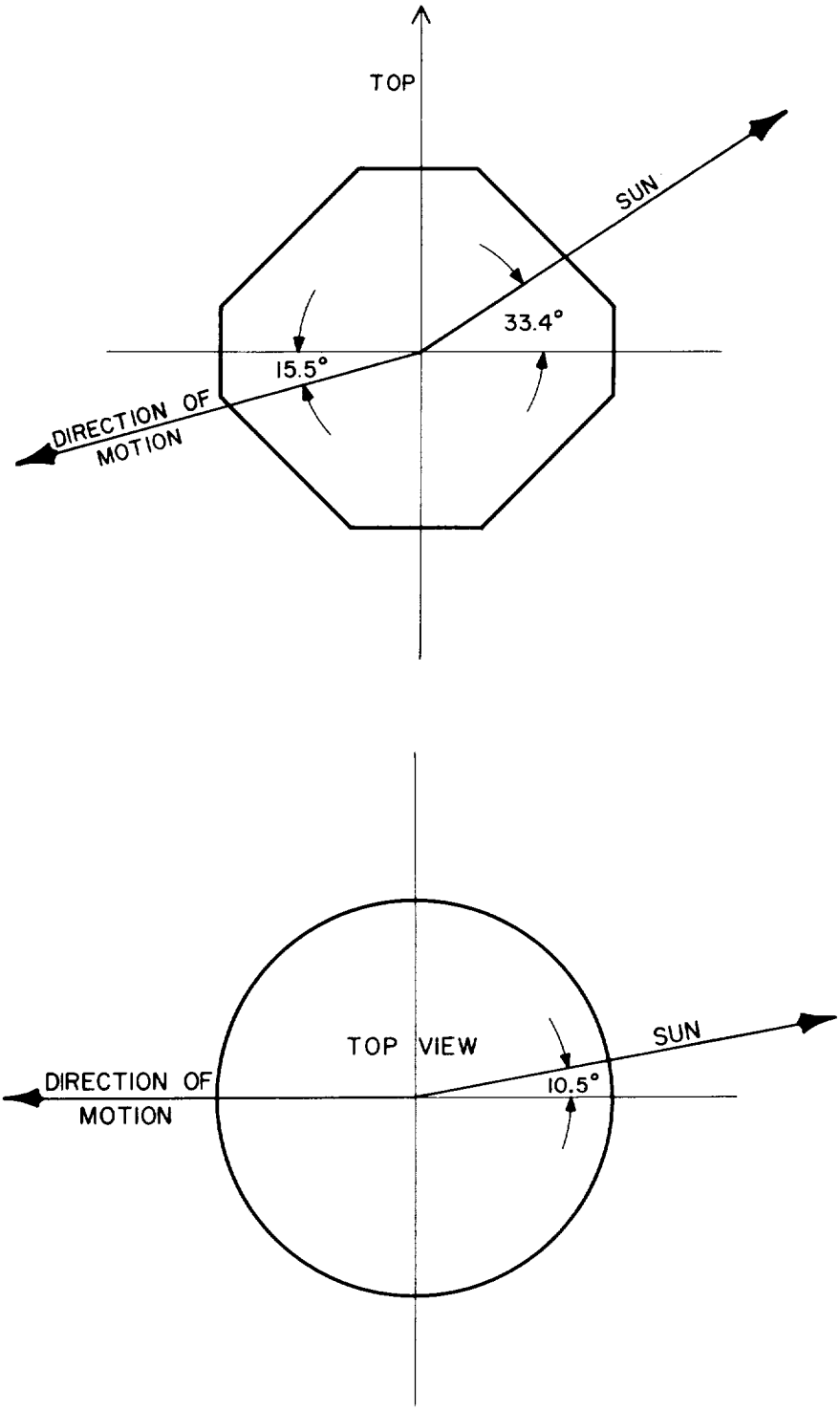

Figure 3 - Satellite orientations (22:57 UT, 27 November 1960)

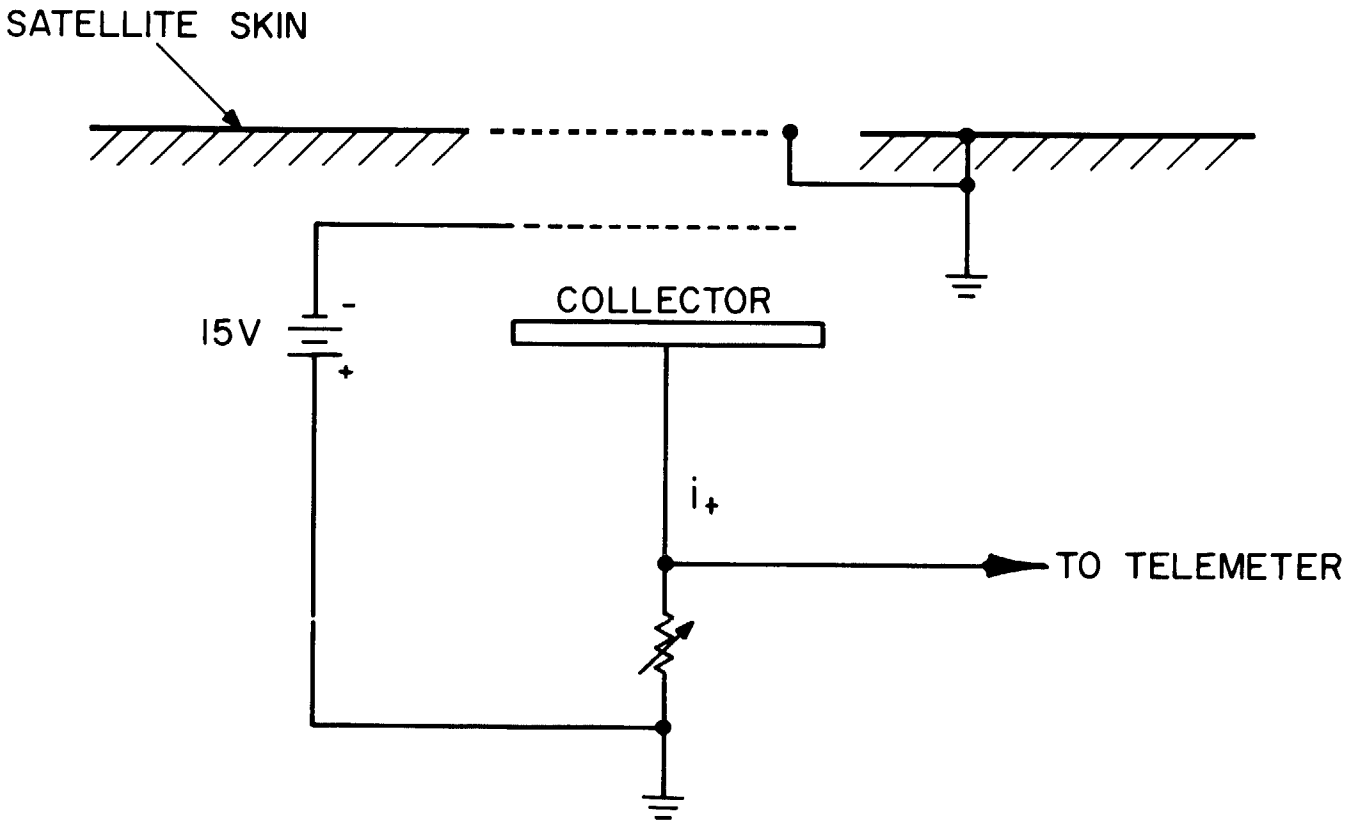

Figure 4 - Ion current monitor

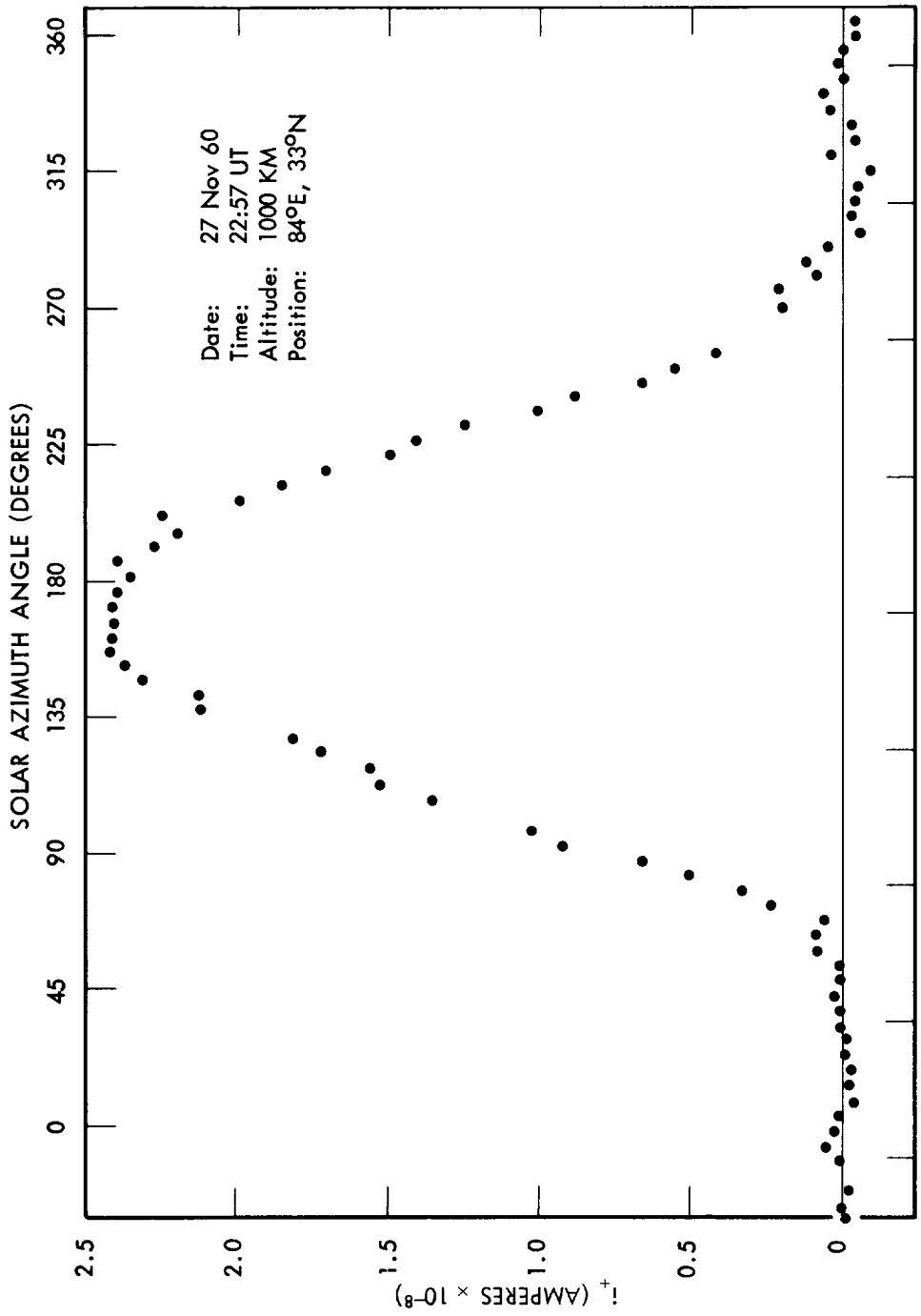

Figure 5 - Ion current as a function of aspect

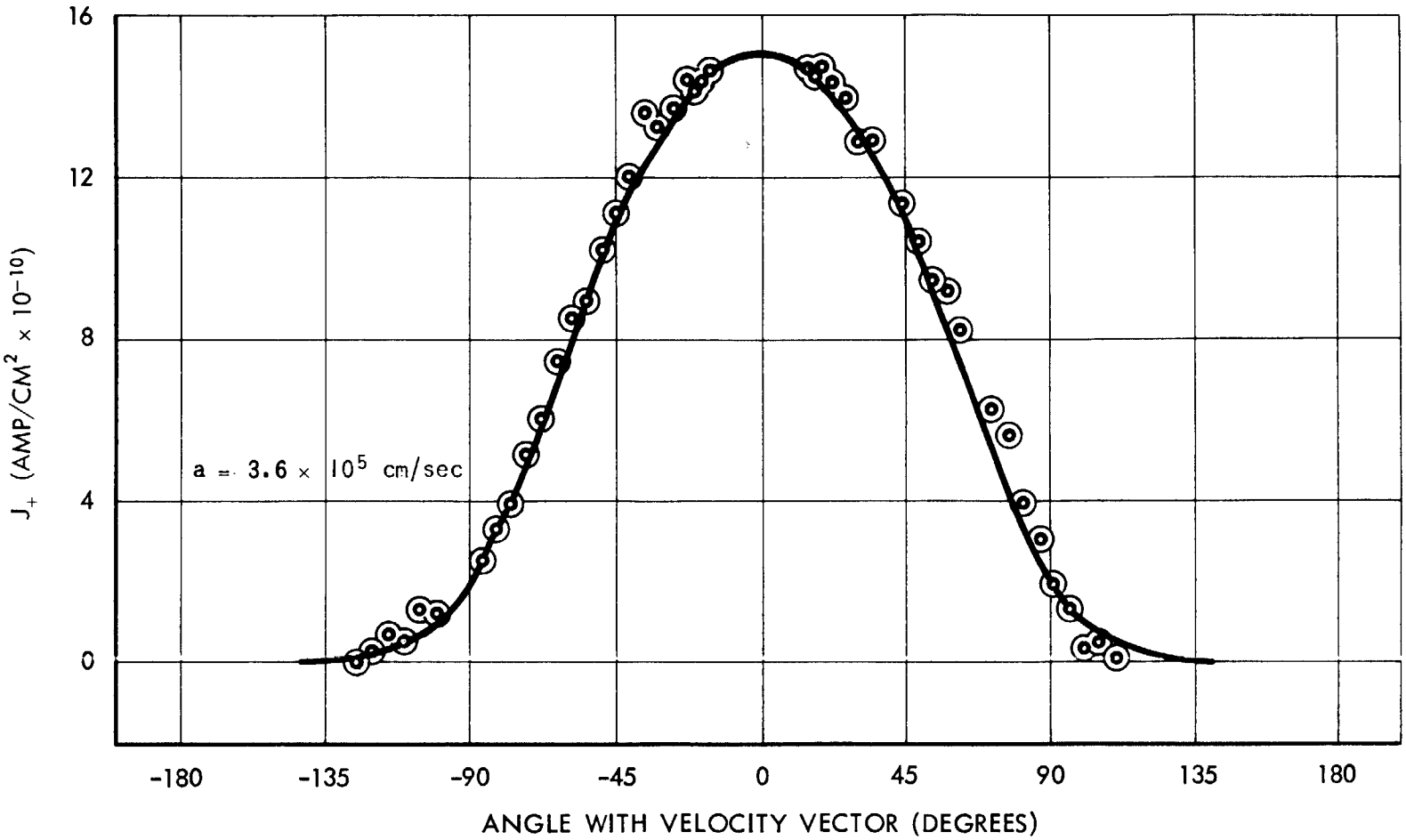

Figure 6 - Variation of positive ion current density with angle relative to satellite velocity vector

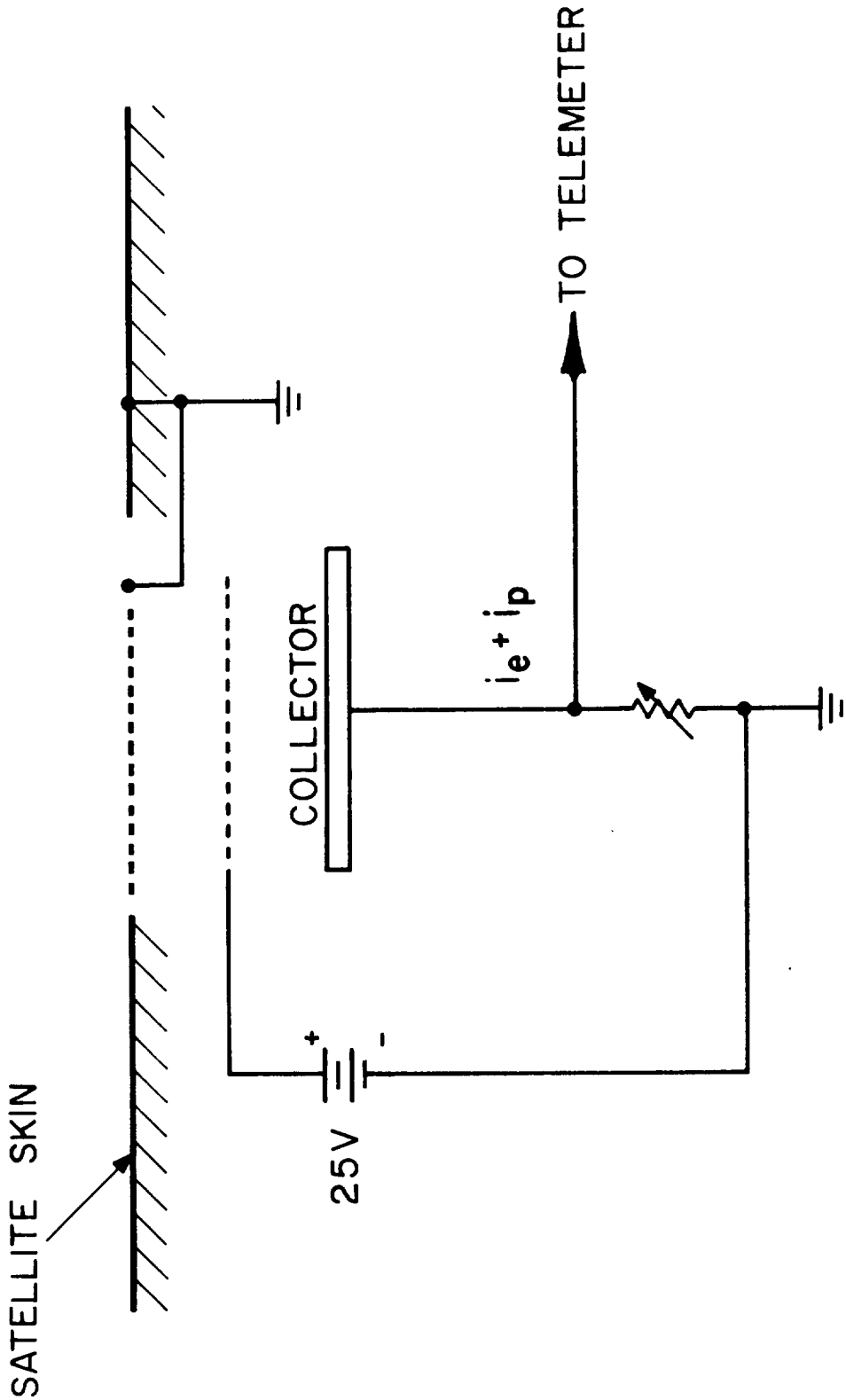

Figure 7 - Electron current monitor

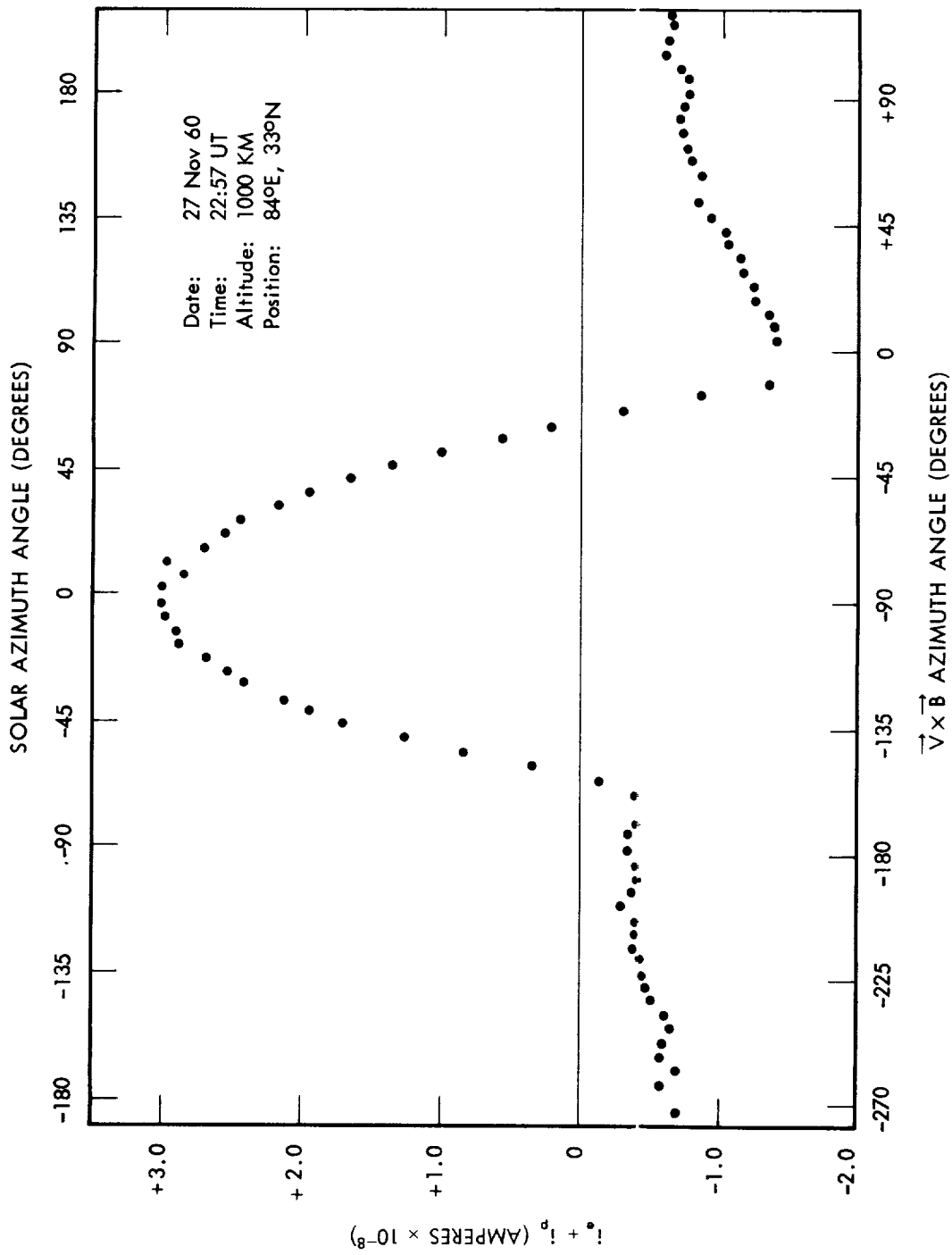

Figure 8 - Electron current as a function of aspect

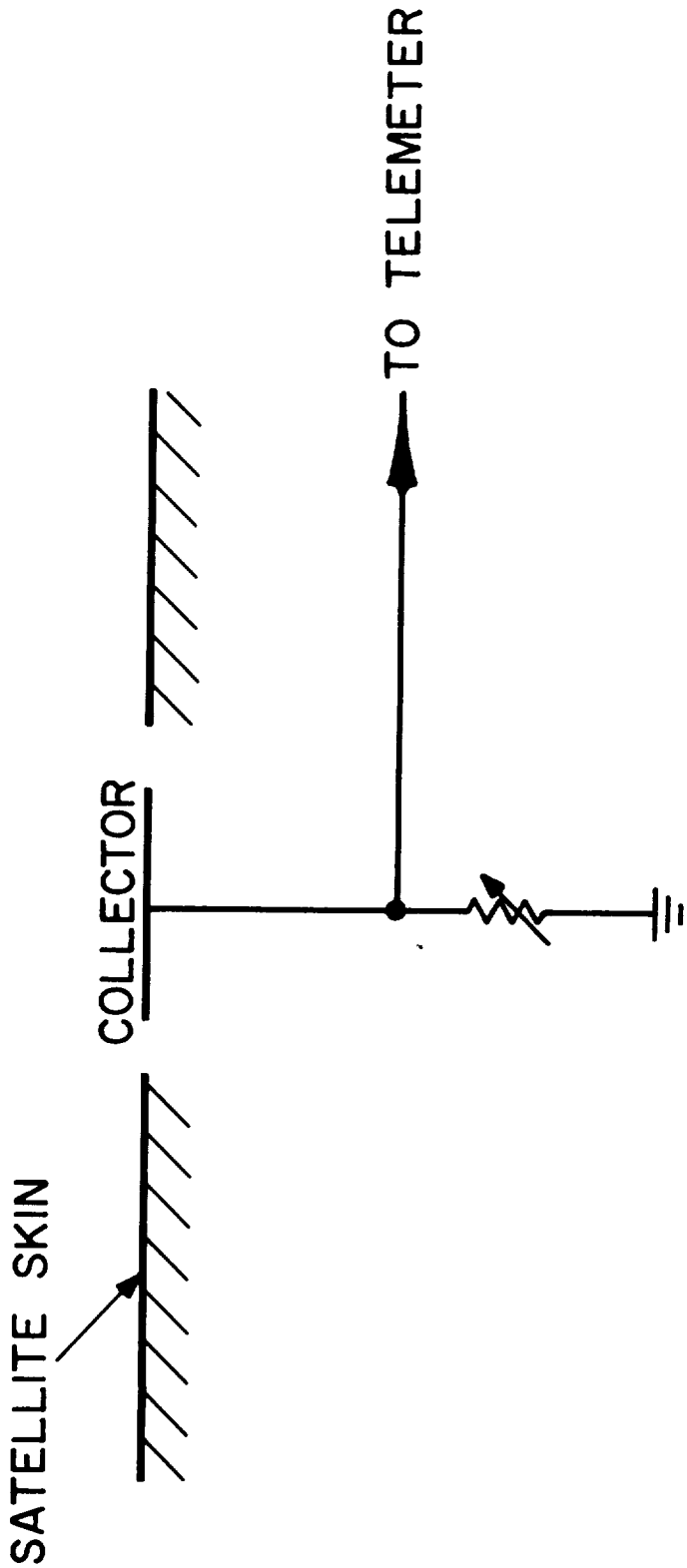

Figure 9 - Total current monitor

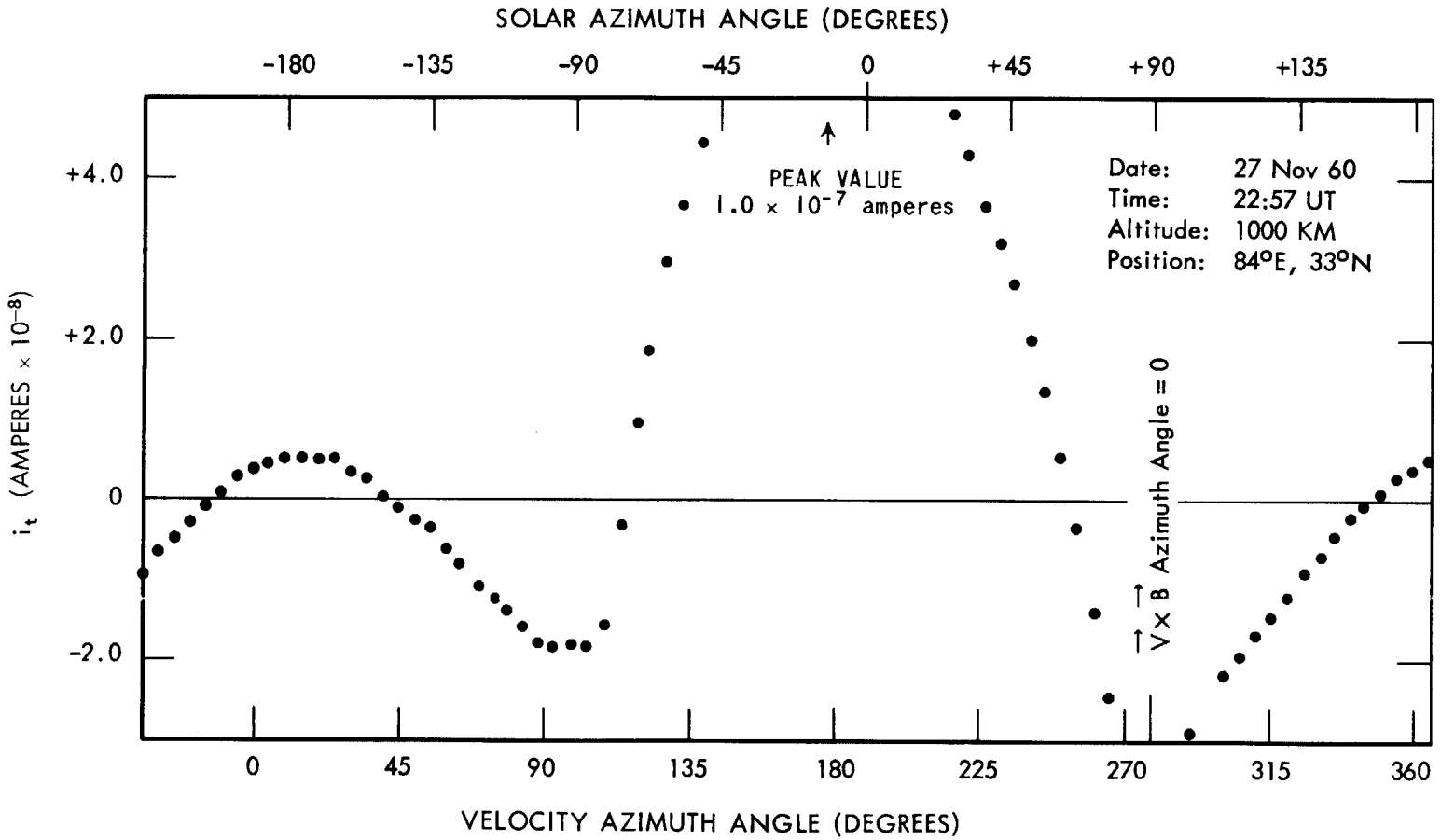

Figure 10 – Total sheath current as a function of aspect

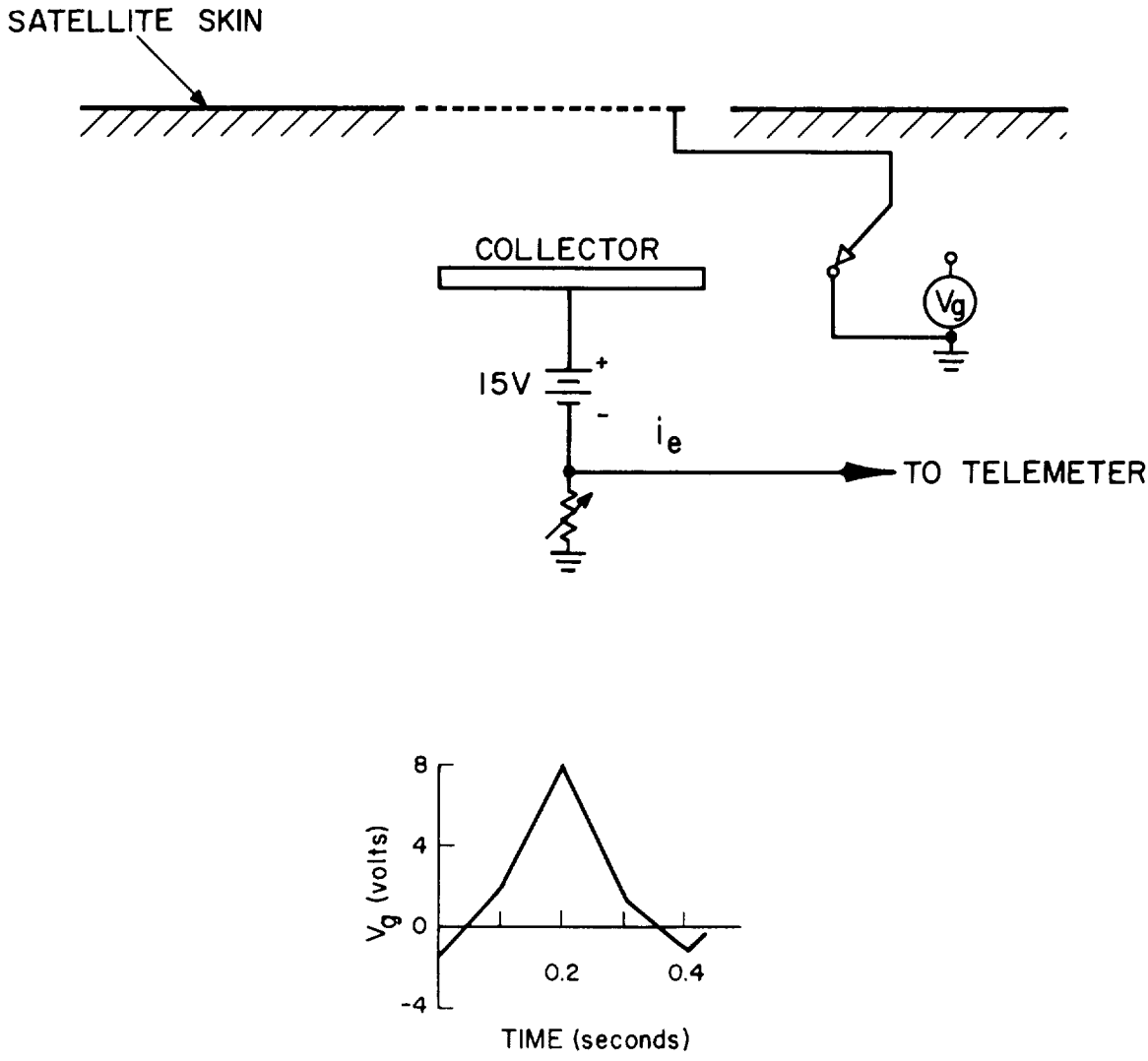

Figure 11 - Electron temperature probe

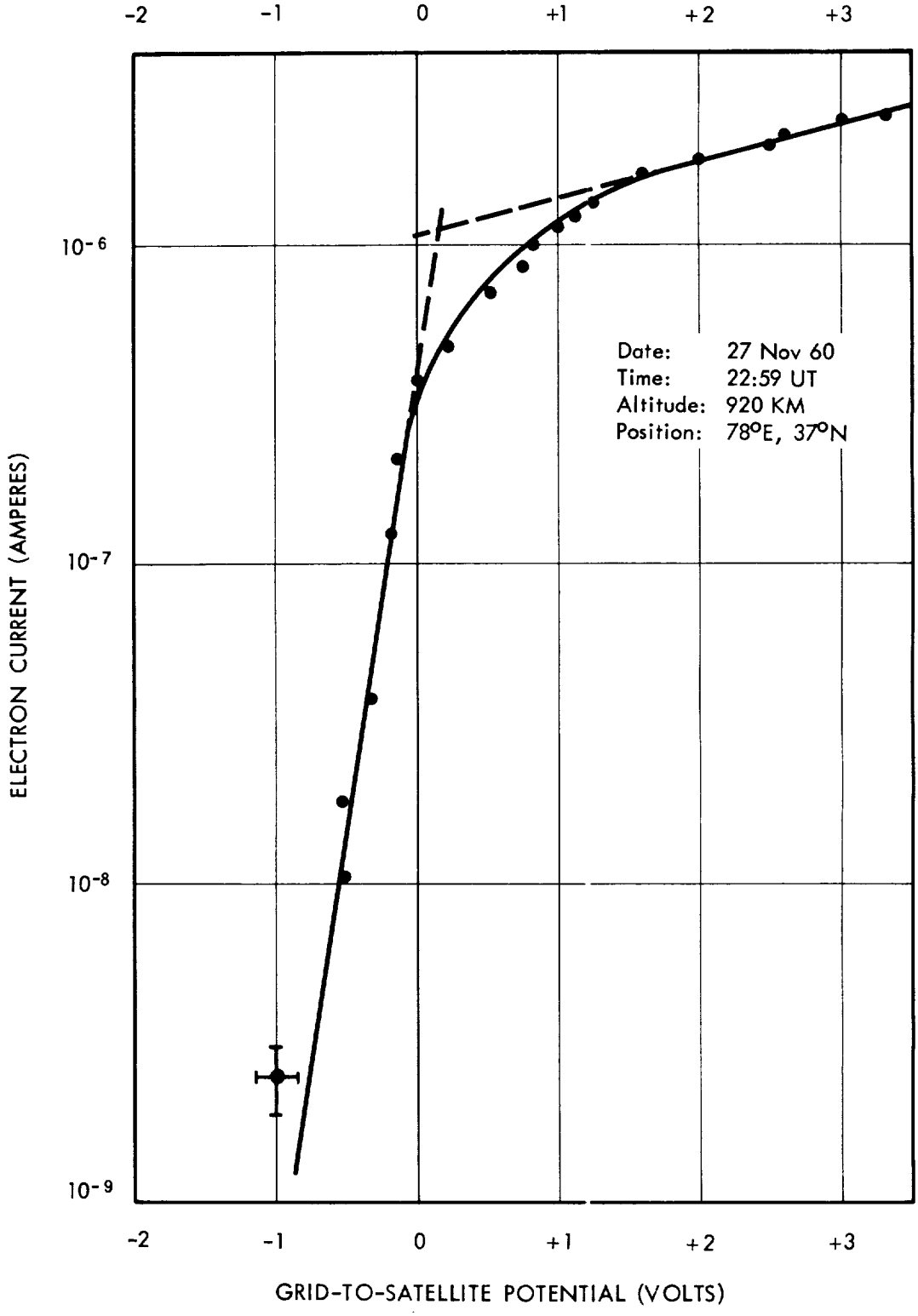

Figure 12 - Typical volt-ampere curve for electron temperature probe

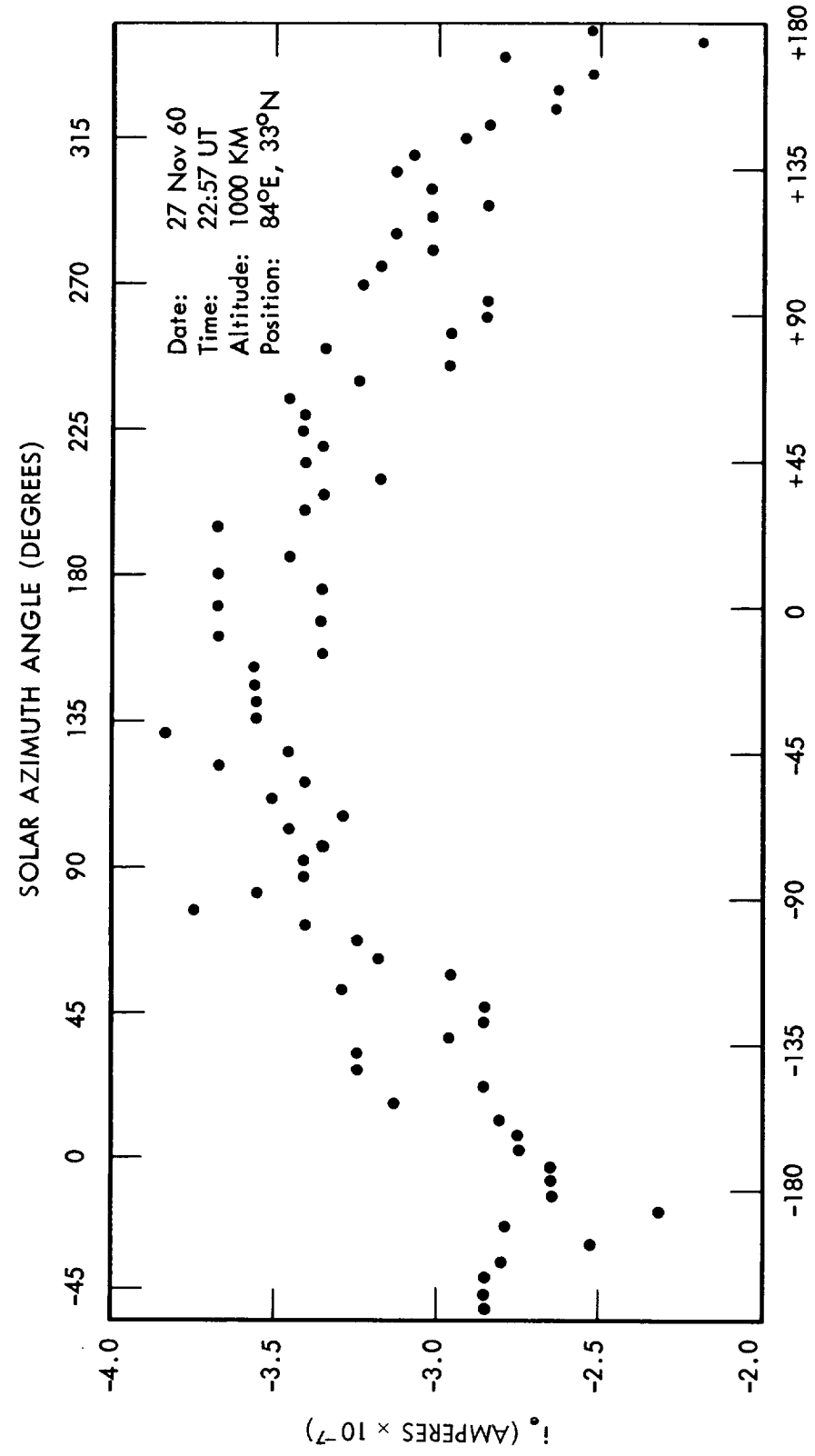

Figure 13 - Electron current as a function of aspect

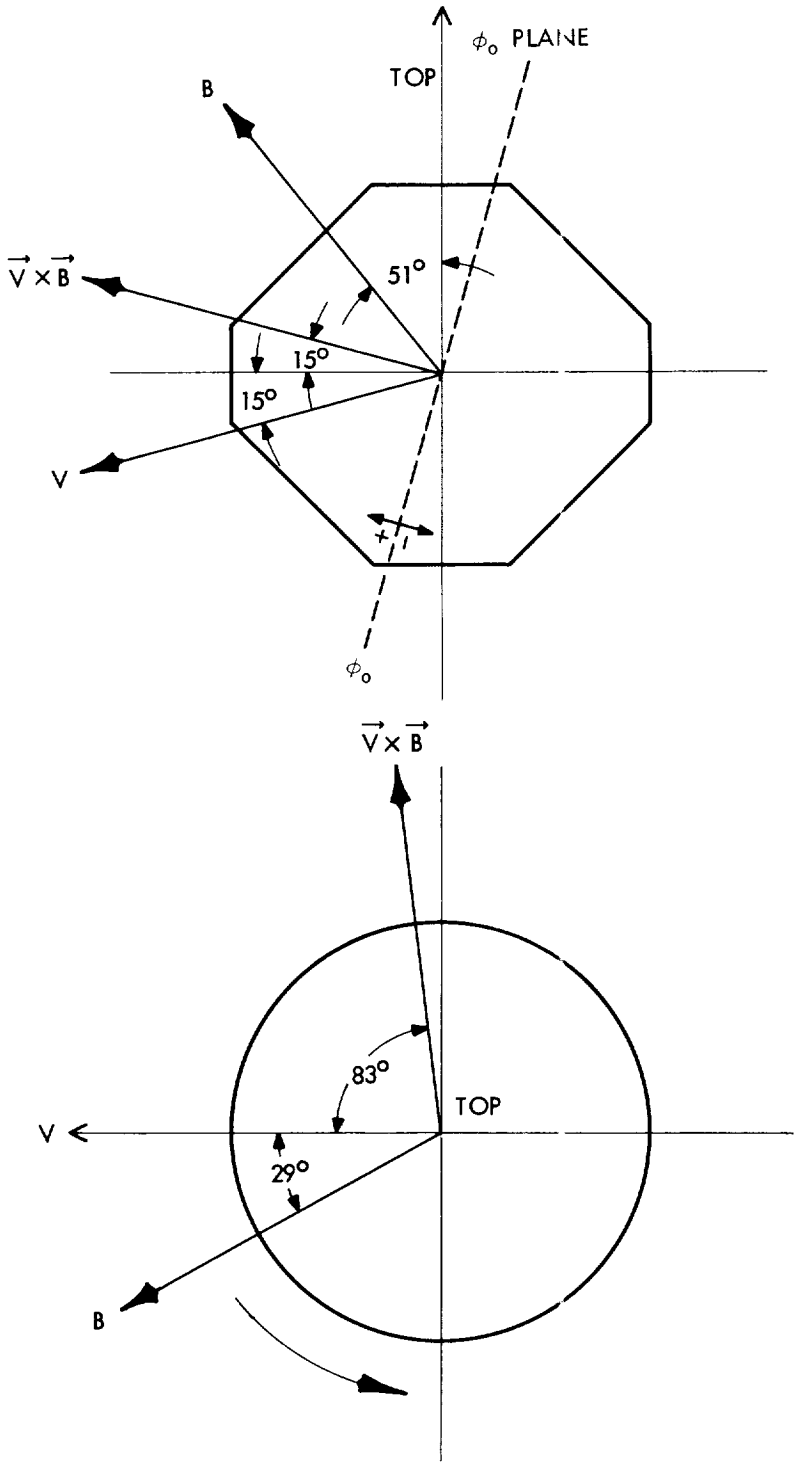

Figure 14 - Orientation of satellite with respect to magnetic and velocity vectors

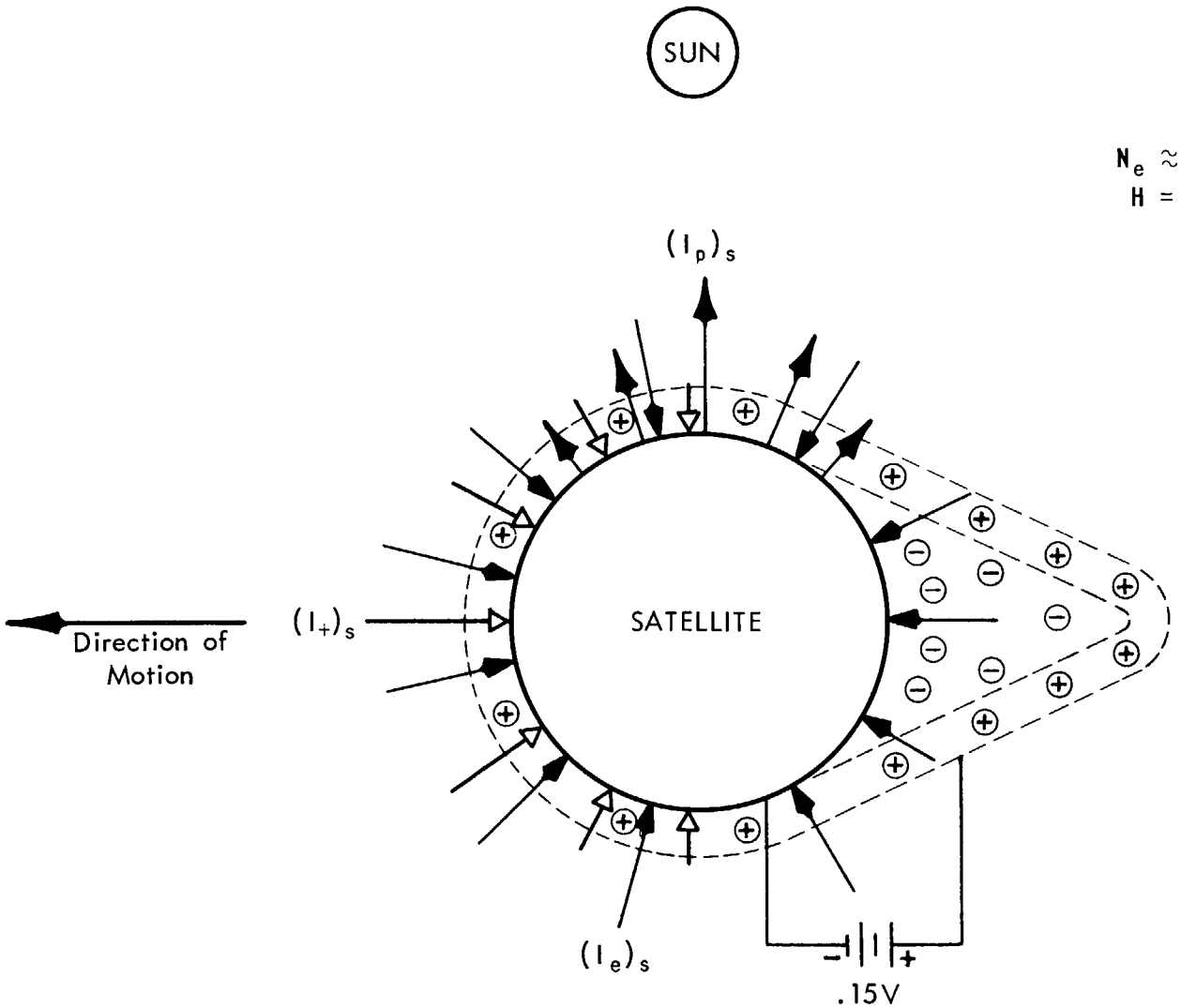

Figure 15 - Qualitative satellite sheath model postulated from experimental data